CANCER

PP2A inhibition is a druggable MEK inhibitor resistance mechanism in KRAS-mutant lung cancer cells

Otto Kauko[1,2,3]*, Caitlin M. O'Connor[4†], Evgeny Kulesskiy[5†], Jaya Sangodkar[6], Anna Aakula[1], Sudeh Izadmehr[6], Laxman Yetukuri[1], Bhagwan Yadav[5], Artur Padzik[1], Teemu Daniel Laajala[5,7], Pekka Haapaniemi[1], Majid Momeny[1], Taru Varila[1], Michael Ohlmeyer[6], Tero Aittokallio[5,7], Krister Wennerberg[5‡], Goutham Narla[4§], Jukka Westermarck[1,2§‖]

Kinase inhibitor resistance constitutes a major unresolved clinical challenge in cancer. Furthermore, the role of serine/threonine phosphatase deregulation as a potential cause for resistance to kinase inhibitors has not been thoroughly addressed. We characterize protein phosphatase 2A (PP2A) activity as a global determinant of KRAS-mutant lung cancer cell resistance across a library of >200 kinase inhibitors. The results show that PP2A activity modulation alters cancer cell sensitivities to a large number of kinase inhibitors. Specifically, PP2A inhibition ablated mitogen-activated protein kinase kinase (MEK) inhibitor response through the collateral activation of AKT/mammalian target of rapamycin (mTOR) signaling. Combination of mTOR and MEK inhibitors induced cytotoxicity in PP2A-inhibited cells, but even this drug combination could not abrogate MYC up-regulation in PP2A-inhibited cells. Treatment with an orally bioavailable small-molecule activator of PP2A DT-061, in combination with the MEK inhibitor AZD6244, resulted in suppression of both p-AKT and MYC, as well as tumor regression in two KRAS-driven lung cancer mouse models. DT-061 therapy also abrogated MYC-driven tumorigenesis. These data demonstrate that PP2A deregulation drives MEK inhibitor resistance in KRAS-mutant cells. These results emphasize the need for better understanding of phosphatases as key modulators of cancer therapy responses.

INTRODUCTION

Critical review of results of a large number of clinical trials indicates that overall, the clinical effectiveness of kinase inhibitors in cancer therapy has not lived up to high original expectations (*1*–*3*). This calls into question whether there is some fundamental lack of understanding of mechanisms that define the efficacy of targeted kinase inhibitor therapies. In particular, targeting RAS–mitogen-activated protein kinase (MAPK) signaling has shown limited success outside melanoma (*2*). Although it is biochemically evident that protein phosphorylation is equally potently regulated by phosphatases as by kinases, the role of phosphatases as determinants of efficacy of phosphorylation targeting therapies is still very poorly understood.

Serine/threonine phosphatase PP2A (protein phosphatase 2A) is a critical human tumor suppressor (*4*, *5*), inhibition of which is a prerequisite for malignant transformation of many types of normal human cells (*5*–*7*) and promotes in vivo tumorigenesis (*8*–*14*). PP2A is an important negative regulator of several oncogenic signaling pathways and particularly of RAS-driven oncogenic signaling (*5*, *7*, *15*, *16*). In full accordance with a requirement of PP2A inhibition for cellular transformation by activated RAS (*6*, *7*), PP2A inhibition promotes malignant growth of various cell types with RAS activating mutations (*15*, *17*). PP2A is a trimeric protein complex in which a core dimer formed by the scaffolding A subunit (PPP2R1A and PPP2R1B) and the catalytic C subunit (PPP2CA and PPP2CB) is associated with one of many B subunits that facilitate and direct the interaction of the trimer with substrate proteins (*5*). Most recurrent cancer-related PP2A mutations are found in the scaffold protein PPP2R1A (*10*, *12*, *18*). Notably, in two independent in vivo lung cancer models, PPP2R1A mutation either increased tumor burden or decreased survival of KRAS-mutant mice (*8*, *10*). In addition, deletions and loss-of-function mutations of PP2A subunits have been reported in patients with lung and other cancers (*5*, *13*). In lung cancers, PP2A activity is also frequently dampened by overexpression of PP2A inhibitor proteins (PIPs) such as CIP2A (*19*) or SET (*17*). Moreover, high expression of CIP2A is synergistic with RAS mutations and expression in correlating with poor survival outcomes across all The Cancer Genome Atlas pan-cancer data (*15*). PP2A and RAS also regulate an overlapping phosphoproteome, providing an additional level of cooperation (*15*). Another PIP, protein phosphatase methylesterase-1 (PME-1), correlates with increased tumor grade in human glioma and enhances malignant growth as well as kinase inhibitor resistance (*20*).

Numerous highly efficient and specific MAPK kinase (MEK) inhibitors (MEKis) have been developed. Their efficacy has been studied in KRAS-mutant lung cancers in a large number of clinical trials, but unfortunately, most patients develop resistance to these agents relatively shortly after therapies have been initiated (*2*, *21*). In addition to mutational mechanisms, clinical inefficacy of MEKi therapies has been attributed to nonmutational rewiring of signaling and particularly MEKi-elicited relief of negative feedback loops at the level of RTKs (receptor tyrosine kinases) and RAF, resulting

[1]Turku Centre for Biotechnology, University of Turku and Åbo Akademi University, 20520 Turku, Finland. [2]Institute of Biomedicine, University of Turku, 20520 Turku, Finland. [3]TuBS and TuDMM Doctoral Programmes, University of Turku, 20520 Turku, Finland. [4]Case Comprehensive Cancer Center, Case Western Reserve University, Cleveland, OH 44106–7285, USA. [5]Institute for Molecular Medicine Finland, University of Helsinki, 00014 Helsinki, Finland. [6]Icahn School of Medicine at Mount Sinai, New York, NY 10029, USA. [7]Department of Mathematics and Statistics, University of Turku, 20520 Turku, Finland.
*Present address: Division of Functional Genomics and Systems Biology, Department of Medical Biochemistry and Biophysics, Karolinska Institutet, SE 171 77 Stockholm, Sweden.
†These authors contributed equally to this work.
‡Present address: Biotech Research and Innovation Centre (BRIC), University of Copenhagen, Copenhagen, Denmark.
§These authors contributed equally to this work.
‖Corresponding author. Email: jukwes@utu.fi

in reactivation of extracellular signal–regulated kinase (ERK) or activation of AKT/mammalian target of rapamycin (mTOR) signaling (*2*, *21*). Inhibition of compensatory RAF activation upon MEKi therapy has shown promising clinical activity, but resistance against these combinations still develops (*2*). Thereby, direct kinase inhibition might need to be combined with alternative strategies that prevent rewiring of signaling in response to the RAF-MEK pathway inhibition. On the basis of the molecular behavior of serine/threonine phosphatases as regulators of protein phosphorylation, they could have an important role in signal rewiring and emergence of collateral kinase inhibitor resistance mechanisms. However, the role of phosphatases in kinase inhibitor responses is very poorly understood, and it is unclear whether deregulated phosphatases could actively drive kinase inhibitor resistance.

RESULTS

PP2A activity is a global determinant of the kinase inhibitor sensitivity of KRAS-mutant lung cancer cells

To evaluate the global relevance of PP2A activity for kinase inhibitor responses in human KRAS-mutant lung cancer cells, we used a previously described drug sensitivity and resistance testing (DSRT) platform (*22*) in KRAS-mutant A549 cells transfected with PPP2R1A, CIP2A, or PME-1 small interfering RNAs (siRNAs). Whereas PPP2R1A depletion models cells with persistent PP2A inhibition (*12*), depletion of PP2A inhibitors CIP2A and PME-1 results in cells with tonally high PP2A activity (*15*, *20*). In support of these concepts, recent studies have demonstrated global serine/threonine dephosphorylation in CIP2A- and PME-1–depleted cells (*23*), and that functional effects of CIP2A and PME-1 depletion can be rescued by concomitant PP2A inhibition (*9*, *20*, *24*). However, because CIP2A and PME-1 do not share structural features and the mechanisms by which they inhibit PP2A activity are vastly different (*25*, *26*), the presumption was that their impacts on kinase inhibitor sensitivity might differ at least to some extent. The third PIP, SET, which has the most prominent effects on PP2A activity based on our recent phosphoproteome screen in HeLa cells (*23*), was excluded from the analysis due to almost complete block of proliferation of A549 cells upon SET siRNA transfection (fig. S1, A and B). Consistent with persistent PP2A inhibition in KRAS-mutant lung cancer cells, SET, PME-1, and CIP2A were overexpressed in various KRAS-mutant lung cancer cell lines as compared to the cyclin-dependent kinase 4 (CDK4) and human telomerase reverse transcriptase (hTERT) immortalized human bronchial epithelial cell line (HBEC; fig. S1C) (*27*).

Each PP2A gene was depleted by three individual siRNAs (fig. S1D), and each kinase inhibitor listed in table S1 was tested over a 10,000-fold concentration range, allowing for the establishment of accurate dose-response curves for each drug in each sample. Differential drug sensitivity scores (ΔDSS), determined by the area under the dose-response curves (*28*), were calculated between the treated and the control samples. The individual drug responses in each of the three conditions are listed in the table S1. All drug responses were ranked by the correlation between ΔDSS and PP2A activity status so that the drugs that exhibited synergy with PP2A reactivation by CIP2A and PME-1 depletion appeared at the top of "correlation rank" (ΔDSS, red), whereas the drugs at the bottom exhibited synergy with PP2A inhibition (ΔDSS, blue). Furthermore, the enrichment scores were calculated for selected drug groups in the ranked list (Fig. 1A). We observed increased kinase inhibitor resistance upon PP2A inhibition, whereas PP2A reactivation resulted in a general sensitization to kinase inhibitors (Fig. 1A and table S1). Volcano plots in Fig. 1B show dependencies of selected drug responses on PP2A modulation. Notably, even though PPP2R1A inhibition predominantly induced drug resistance, and CIP2A and PME-1 depletion predominantly induced drug sensitization, in each case the opposite patterns were also observed. As an example, PPP2R1A inhibition very potently sensitized cells to the PKC (protein kinase C) activator bryostatin, whereas both CIP2A and PME-1 inhibition induced resistance to BCL2 (B cell lymphoma 2) inhibitors (Fig. 1B). Thereby, our results suggest a global relevance of PP2A biology for kinase inhibitor responses but also argue for specific interactions between different PP2A complexes and individual drug families.

Clear PP2A dependencies were observed for MEK/ERK, epidermal growth factor receptor (EGFR), and Aurora kinase (AURK) inhibitors (Fig. 1, C to E; drug sensitivity data for three individual siRNAs per gene are shown in fig. S1E). The depletion of PPP2R1A conferred resistance to MEKis, whereas CIP2A and PME-1 depletions as a group resulted in a statistically significant MEKi sensitization ($P = 0.002$ for combination and $P = 0.02$ for CIP2A alone; Fig. 1C and table S1). PPP2R1A inhibition also induced marked resistance to two ERK inhibitors in the library (Fig. 1C). On the other hand, depletion of either CIP2A or PME-1 sensitized the cells to EGFR inhibitors, whereas depletion of PPP2R1A had no effect on average (Fig. 1D). Similar responses with CIP2A and PME-1 argue for regulation of shared PP2A targets implicated in EGFR inhibitor response, whereas lack of effect of PPP2R1A inhibition may indicate that these targets are already fully phosphorylated due to CIP2A- or PME-1–mediated PP2A inhibition. The AURK inhibitors exhibited yet another distinctive profile of PP2A dependency, where resistance caused by PPP2R1A inhibition and sensitization caused by PME-1 depletion support PP2A dependence (Fig. 1E). However, selective sensitization by PME-1 but not by CIP2A depletion (Fig. 1E) may be explained both by the nonoverlapping PP2A targets regulated by PME-1 and CIP2A (*23*) and by nuclear colocalization of PME-1 (*29*, *30*) and AURK targets (*31*), whereas CIP2A is mostly cytoplasmic (*30*, *32*).

The results for the 18 selected kinase inhibitors covering the most PP2A-dependent kinase families (Fig. 1A and table S2) were concordant between A549 and another KRAS-mutant lung cancer cell line, NCI-H2122 (Fig. 1, F and G, and table S2). In contrast, NCI-H460 cells exhibited divergent and, on average, smaller-magnitude responses (Fig. 1, F and G, and table S2). In addition to KRAS mutation, NCI-H460 also harbors a homozygous loss-of-function PPP2R1A mutation (E64D), making it most likely resistant to PP2A modulation by PME-1 and CIP2A depletion. This genetic evidence further corroborates the functional link between PP2A inhibition and overall kinase inhibitor resistance.

The PPP2R1A E64D mutation found in NCI-H460 cells contributes to RAS-driven lung cancer progression (*10*). Although it is not directly linked to the kinase inhibitor resistance phenotype described in this study, we observed that clustered regularly interspaced short palindromic repeats (CRISPR)/CRISPR-associated protein 9 (Cas9)–mediated reversal of a single PPP2R1A-mutant allele caused a significant growth arrest phenotype in this cell line ($P = 0.0053$; fig. S1, F and G). The growth arrest can be explained at least partly by a senescence phenotype observed in these cells (Fig. 1,

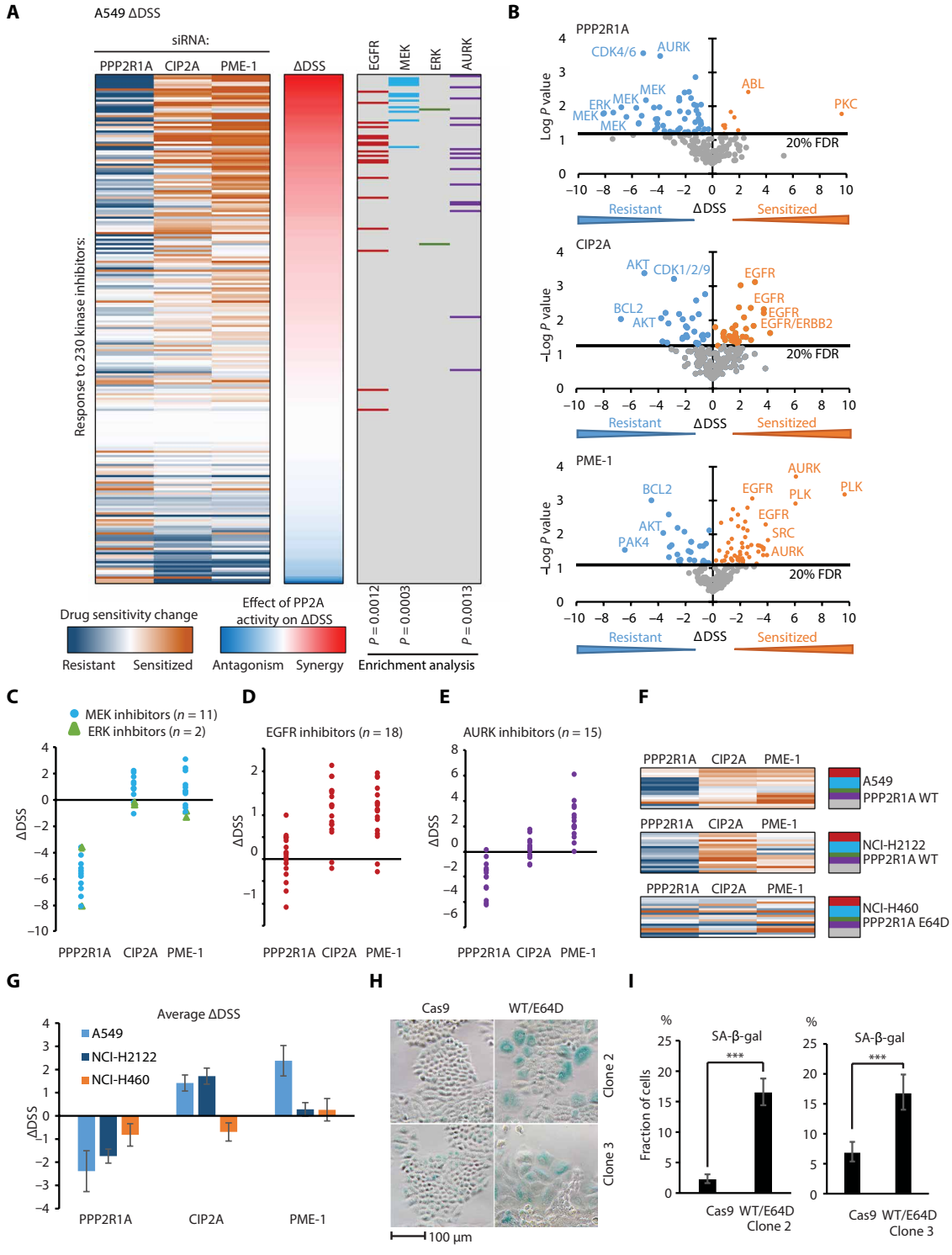

Fig. 1. PP2A inhibition drives kinase inhibitor and senescence resistance in KRAS-mutant lung cancer cells. (**A**) Drug sensitivities to 230 kinase inhibitors in A549 cells transfected with indicated siRNAs in triplicates (three siRNAs per gene) were measured by cell viability assay. The drug responses are ranked by ΔDSS, which quantifies the difference between cells with PP2A inhibition (PPP2R1A siRNA) and PP2A activation (CIP2A and PME-1 siRNAs). Statistically significant enrichment for differential sensitivity to certain inhibitor families is shown in the right. *P* values for enrichment were calculated similarly to Gene Set Enrichment Analysis (GSEA), as described in Materials and Methods. (**B**) Volcano plots showing the differential sensitivity of A549 cells to drugs for each condition based on data shown in (A). *P* values were calculated by two-tailed *t* test for each drug tested in three biological replicates, and the 20% false discovery rate (FDR) was determined by Benjamini-Hochberg correction. (**C** to **E**) Impact of PP2A modulation on ΔDSS in A549 cells treated with (C) MEKi (n = 11; blue dots) and ERK inhibitors (n = 2; green triangles), (D) EGFR inhibitors (n = 18), or (E) AURK inhibitors (n = 15). Data are extracted from (A) and shown as mean values for three replicate experiments with different siRNAs. (**F**) Responses of A549 cells and two other KRAS-mutant cell lines, NCI-H2122 and NCI-H460, with the indicated PPP2R1A genetic status to selected kinase inhibitors listed in table S2. Color coding of responses follows the same as in (A). (**G**) Average responses from (F). Data are shown as means ± SEM for 18 drugs. (**H**) Senescence-associated β-galactosidase (SA-β-gal) staining in two individual NCI-H460 clones after reverting one allele of the homozygous PPP2R1A E64D mutation back to wild-type (WT) sequence. (**I**) Fraction of β-galactosidase stain–positive and flattened cells ± 95% confidence intervals was calculated for pooled data from seven and five technical replicates, respectively, for clones 2 and 3 and their corresponding controls. ***$P < 0.001$ for χ^2 test.

H and I, and fig. S1H). Senescence induction by PP2A reactivation is consistent with in vivo senescence induction in a CIP2A-deficient HER2$^+$ breast cancer mouse model (*9*) and with the role of the PP2A target protein MYC (fig. S1B) (*24*, *32*, *33*) in senescence evasion in KRAS-mutant cells (*34*).

We conclude that PP2A globally affects kinase inhibitor sensitivity in KRAS-driven lung cancer cells. Moreover, growth arrest after CRISPR-mediated reversal of one PPP2R1A-mutant allele in NCI-H460 cells indicates that KRAS-driven cancer cells may depend on constitutive PP2A inhibition.

PP2A inhibition confers MAPK pathway inhibitor resistance in KRAS-mutant lung cancer cells

The results above indicate that PP2A inhibition drives MEKi resistance in KRAS-mutant cells. Trametinib (MEKi) resistance in PPP2R1A-depleted cells was validated using cell viability and colony formation assays (Fig. 2, A to C). Although PPP2R1A depletion reportedly reduced the colony formation ability of cells (*12*), it also granted a selective advantage under trametinib treatment (Fig. 2, B and C). The gene-dose dependency of resistance to trametinib was evident in A549 cells, in which one or two of four PPP2R1A alleles were knocked out using CRISPR/Cas9 (Fig. 2, D and E). Moreover, NCI-H460 cells with PPP2R1A mutations were less sensitive to trametinib (Fig. 2F), whereas CRISPR/Cas9 clones with WT/E64D PPP2R1A genotype exhibited increased trametinib sensitivity (fig. S2, A and B). Notably, PPP2R1A-dependent trametinib resistance was already observed with subnanomolar trametinib concentrations, which have no significant cell killing activity in cell viability assays (fig. S2, A, C, and D), indicating that PP2A inhibition targets cellular signaling activity mechanisms rather than general cell survival mechanisms. Because inhibition of PPP2R5 (B56) PP2A complexes by CIP2A overexpression (*26*) or decreased expression of the PPP2R2 (B55) family subunits (*35*) is a potential mechanism of PP2A inhibition in human lung cancer cells, we further tested the contributions of both of these PP2A subunit families to trametinib sensitivity. For this purpose, H358 cells were stably transduced with short hairpin RNAs (shRNAs) against all PPP2R5 and PPP2R2 subunits. The inhibition of PPP2R5B, PPP2R5E, and all PPP2R2 subunits resulted in a trametinib resistance in colony growth assays (Fig. 2G and fig. S2, E to G). Together, these results establish a causal relationship between PP2A inhibition and trametinib resistance.

The release of negative ERK-RAF feedback regulation is an important MEKi resistance mechanism (*2*). This was evidenced by transition of cytostatic trametinib response in control A549 cells (Fig. 2, A and F) to cytotoxic response upon cotreatment with pan-RAF inhibitor LY3009120 (Fig. 2H). The cytotoxicity of LY3009120/trametinib combination in the control cells was confirmed by a dose-dependent induction of caspase-3/7 activity (fig. S2H). However, PPP2R1A depletion desensitized A549 cells to LY3009120/trametinib combination in both cell viability and colony formation assays (Fig. 2, H and I). PP2A inhibition not only shifted the dose-response pattern of cotreated cells (Fig. 2H) but also prevented the effect of the LY3009120/trametinib combination in colony growth inhibition (Fig. 2I). These results demonstrate that PP2A inhibition confers resistance of KRAS-mutant lung cancer cell lines to MAPK inhibition, including the clinically relevant combination of MEKi and RAFi.

AKT/mTOR signaling is a collateral MEKi resistance mechanism in PPP2R1A-depleted cells

To characterize PPP2R1A-mediated MEKi resistance at the phospho-target level, we used mass spectrometry (MS)–based phosphoproteomics in PPP2R1A-depleted and trametinib-treated A549 cells. PPP2R1A depletion increased the phosphorylation of a subset of ERK targets (>2-fold up-regulation, n = 23/105), and these PPP2R1A-regulated sites were not down-regulated in cells treated with trametinib alone (Fig. 3A and fig. S3A). Conversely, trametinib-sensitive sites (>2-fold down-regulation, n = 19) were not up-regulated by PPP2R1A depletion (Fig. 3A and fig. S3A). Thus, PPP2R1A depletion and trametinib were found to largely regulate different ERK targets. Moreover, although trametinib prevented the up-regulation of some of the phosphorylation induced by PPP2R1A depletion, PPP2R1A depletion was unable to rescue the effect of trametinib on ERK targets (Fig. 3A and fig. S3A). This indicates that the resistance to trametinib caused by PPP2R1A depletion cannot be explained by regulation of ERK pathway activity but is mediated by the activation of ERK-independent collateral pathways.

We examined the role of AKT/mTOR signaling as a candidate collateral MEKi resistance mechanism in PPP2R1A-depleted cells. This was based on previously published evidence of both AKT and mTOR as PP2A target pathways (*15*, *18*), including association of PP2A inhibition with mTOR/S6 activation in human salivary gland tumors (*30*). Reanalysis of the phosphoproteomics data demonstrated a clear shift toward increased expression of phosphorylated AKT (p-AKT) targets in PPP2R1A-depleted A549 cells that were treated with trametinib (striped area in Fig. 3B). Western blot analysis showed a robust increase in phosphorylation of both S6K and S6 in PPP2R1A-depleted cells, whereas PP2A inhibition alone did not result in evident increase in phosphorylation of AKT (Fig. 3C). However, consistent with the phosphoproteomics analysis, PPP2R1A inhibition potentiated trametinib-induced expression of p-AKT (Fig. 3C). Hyperphosphorylation of AKT substrate motifs and S6 was also confirmed in PPP2R1A-depleted HeLa cells (fig. S3B).

These results suggest that PPP2R1A inhibition potentiates collateral activation of AKT/mTOR signaling upon trametinib treatment rather than affecting the direct MEK-ERK pathway targets. Consistent with our model, increased MEK inhibition caused PPP2R1A-depleted cells to be increasingly AKT-dependent. This was demonstrated by partial reversal of resistance in the presence of perifosine (AKT inhibitor) in the cells with maximal MEK inhibition (Fig. 3D). Dependence on AKT/mTOR signaling was even more evident in cells treated with a combination of trametinib and the mTOR inhibitor temsirolimus. Although PP2A inhibition caused resistance to the trametinib + temsirolimus combination (Fig. 3, E and F), increased trametinib concentration resulted in an increased dependence of PPP2R1A-depleted cells on mTOR activity. With the highest concentration of trametinib, cytotoxicity was also reached in those cells (Fig. 3, E and F, red circle). These results were further confirmed by using the dual AKT/mTOR inhibitor BEZ235 in combination with trametinib. BEZ235 increased the trametinib response of PPP2R1A-depleted cells in a colony growth assay (fig. S3, C and D). In a short-term cell viability assay, PPP2R1A inhibition conferred a resistance to BEZ325 in combination with sublethal trametinib concentration (fig. S3E). Our data thus indicate that PP2A inhibition drives MEKi resistance at least by potentiation of collateral activation of AKT/mTOR activity.

We validated our findings using ERK, AKT, and mTOR pathway-related phospho-antibodies. Trametinib blocked both basal and PPP2R1A depletion–induced phosphorylation of ERK, S6K, and glycogen synthase kinase 3 beta (GSK3B) (Fig. 3G). However, even though trametinib inhibited phosphorylation of S6 in the basal conditions, it could not prevent increase in the phosphorylation of S6 in PPP2R1A-depleted cells, indicating a direct PP2A-mediated dephosphorylation of S6 (Fig. 3G). The cytotoxic effects of the trametinib + temsirolimus combination in PPP2R1A-depleted cells were associated with inhibition of phosphorylation of S6K, S6, and AKT (Fig. 3G), providing a mechanistic basis for reversal of PP2A inhibition-induced MEKi resistance. Temsirolimus could not, however, reverse the increase in phosphorylation of GSK3B or expression of MYC in PPP2R1A-depleted cells, even when used in combination

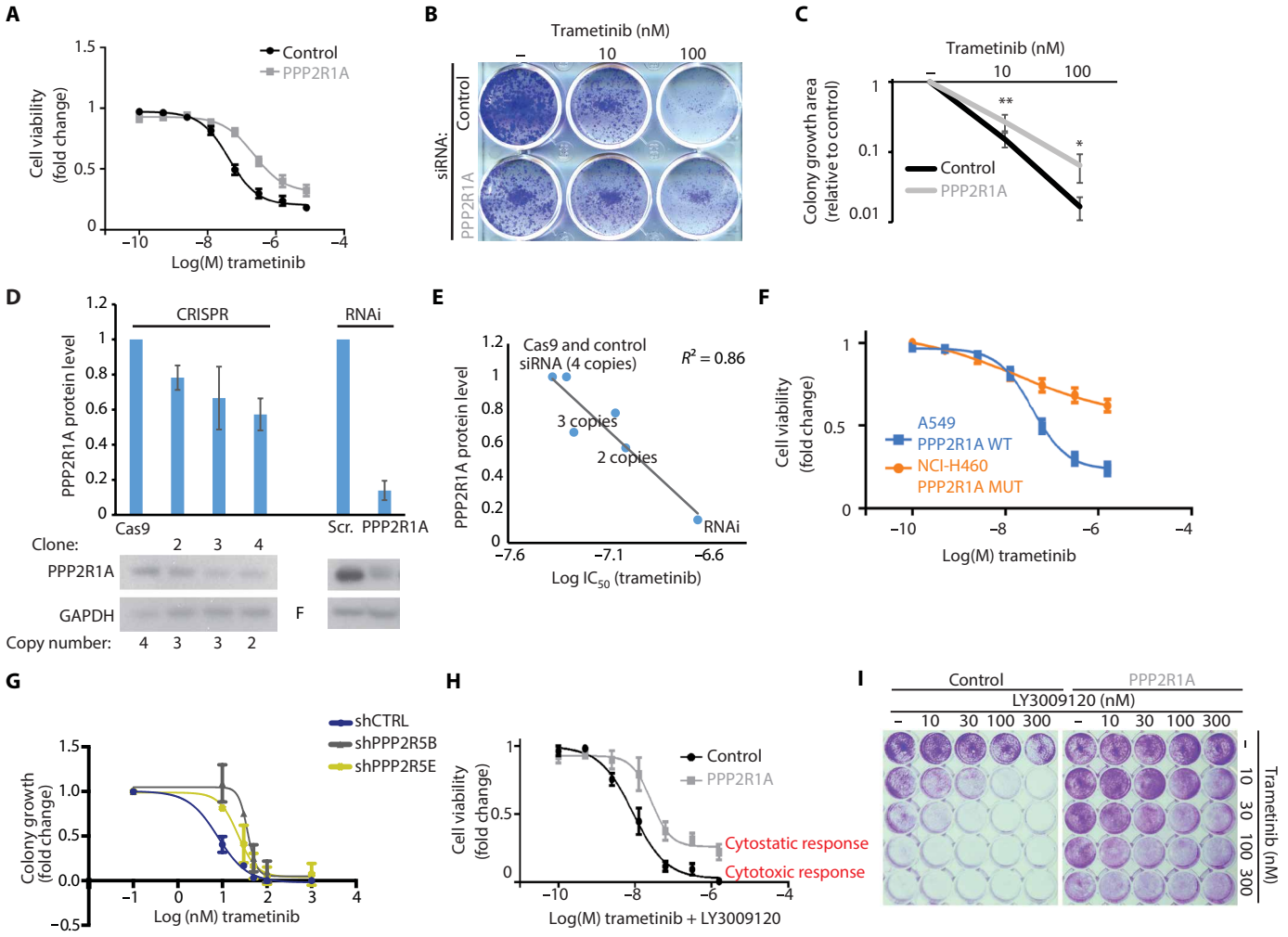

Fig. 2. PP2A inhibition confers MAPK pathway inhibitor resistance in KRAS-mutant lung cancer cells. PPP2R1A denotes RNA interference (RNAi)–mediated silencing of PPP2R1A in each panel. (**A**) Trametinib dose-response curve of A549 cells transfected with either control or PPP2R1A siRNA. Data are shown as means ± SEM for 11 biological replicate experiments with three technical replicates. (**B**) Colony formation assay for trametinib-treated A549 cells transfected with either scrambled or PPP2R1A siRNA. (**C**) Impact of PPP2R1A inhibition in trametinib response in colony formation assay. $^{**}P < 0.01$, $^{*}P < 0.05$, two-tailed *t* test. Data are shown as means ± SEM for six biological replicate experiments. (**D**) PPP2R1A protein content in control A549 cells (with four PPP2R1A alleles) or in cell clones in which CRISPR/Cas9 had selectively deleted one or two copies of the *PPP2R1A* gene. As a control, PPP2R1A expression was also inhibited by RNAi. Data are shown as means ± SEM for five biological replicate experiments. Scr., scramble; GAPDH, glyceraldehyde-3-phosphate dehydrogenase. (**E**) Pearson's correlation ($P = 0.0076$) between cell viability log[IC_{50} (half maximal inhibitory concentration)] for trametinib (eight biological replicate experiments with three technical replicates for the knockouts) and PPP2R1A protein expression based on (D). (**F**) Comparison of trametinib sensitivity of A549 (PPP2R1A WT) and NCI-H460 (PPP2R1A MUT) cells. Data are shown as means ± SEM for 11 biological replicate experiments with three technical replicates. (**G**) Dose-response curve of a clonogenic assay of H358 cells with shRNA knockdown of PPP2R5 (B56) family proteins or control vector (shCTRL). The graph represents the mean colony number ± SD relative to the vehicle control, three biological replicates with two technical replicates. For clarity, only shB56 knockdown lines, shPPP2R5B (gray) and shPPP2R5E (green), which have decreased sensitivity to trametinib, are shown in addition to the control. The cell colonies and data for other PPP2R5 shRNAs are shown in fig. S2 (E and F). (**H**) Cell viability assay of either scrambled or PPP2R1A siRNA–transfected A549 cells treated with increasing doses of trametinib and RAF inhibitor LY3009120. Data are shown as means ± SEM for three replicate experiments. (**I**) Colony formation assay of scrambled or PPP2R1A siRNA–transfected A549 cells treated with increasing concentrations of trametinib and RAF inhibitor LY3009120 either alone or in combination.

with trametinib (Fig. 3, G and H). This may be an important finding in the light of recent data indicating that MYC inhibition is required for clinical efficiency of MEK/ERK inhibition (*34*). In support of this conclusion, stable overexpression of MYC in H358 cells conferred trametinib resistance in a colony growth assay (Fig. 3I). The role of MYC as a critical PP2A target in KRAS-mutant cells was further indicated by potent growth arrest and MYC inhibition in SET-depleted A549 cells (fig. S1, A and B).

We conclude that cancerous PP2A inhibition drives MEKi resistance via collateral activation of AKT and mTOR/S6K signaling. The data also indicate that PP2A inhibition–induced MYC expression is refractory to MAPKi combination therapy, and therefore, it may eventually contribute to tumor relapse.

Pharmacological PP2A reactivation potentiates the therapeutic effect of MEK inhibition

To demonstrate the translational impact of PP2A inhibition as a MEKi resistance mechanism, we tested potential combinatorial activity of recently published orally bioavailable small-molecule activators of PP2A (SMAPs) (*11*) and MEKi in KRAS-mutant lung cancer

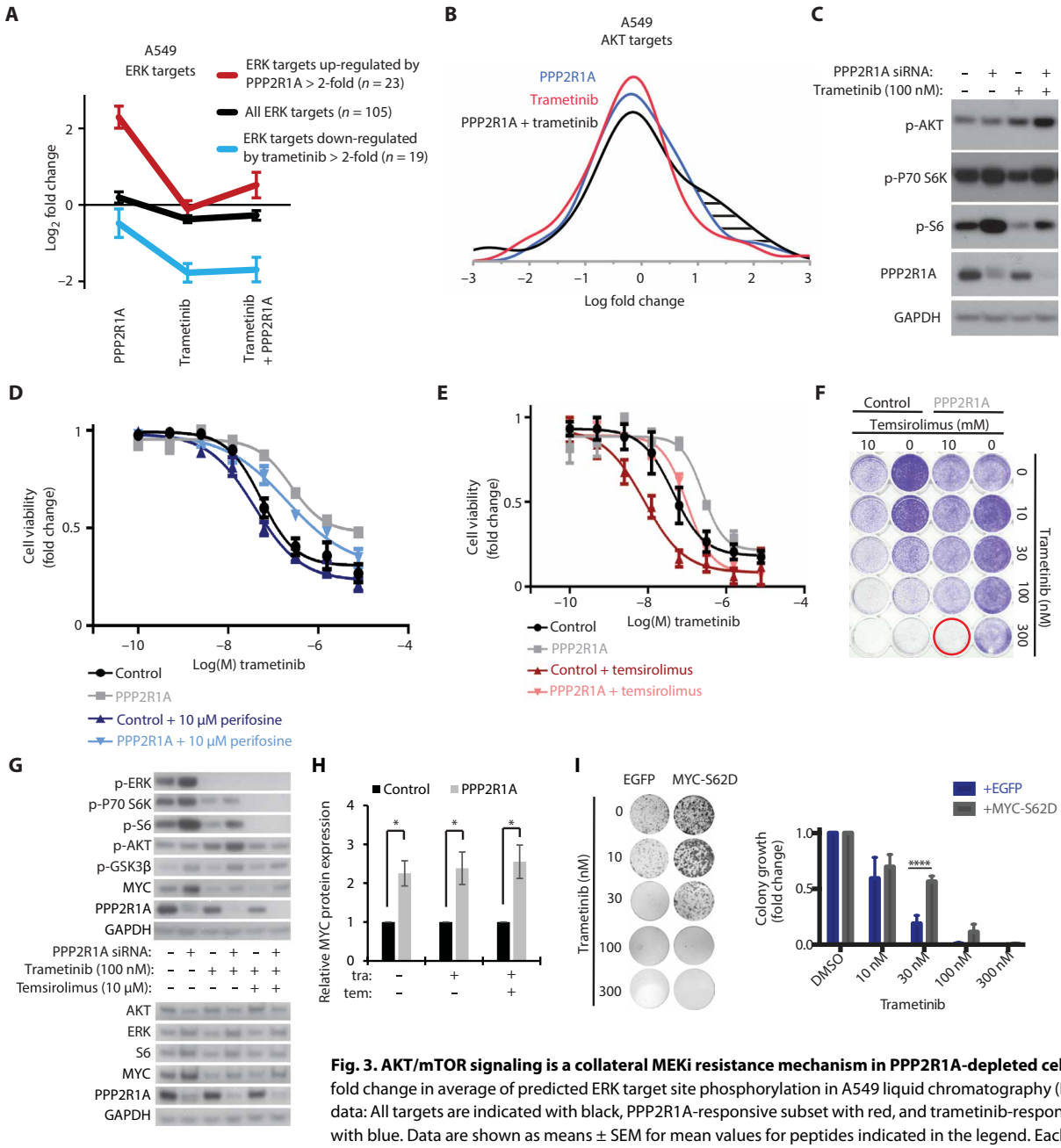

Fig. 3. AKT/mTOR signaling is a collateral MEKi resistance mechanism in PPP2R1A-depleted cells. (**A**) Log_2 fold change in average of predicted ERK target site phosphorylation in A549 liquid chromatography (LC)–MS/MS data: All targets are indicated with black, PPP2R1A-responsive subset with red, and trametinib-responsive subset with blue. Data are shown as means ± SEM for mean values for peptides indicated in the legend. Each condition was analyzed as three biological replicates with different siRNA sequences (**B**) LC-MS/MS data of phosphorylation of AKT targets in cells treated as indicated. The shaded area highlights the shift in AKT target phosphorylation in PPP2R1A siRNA–transfected cells treated with trametinib. Distribution of mean log fold changes for three biological replicate experiments is shown. (**C**) Western blot analysis of selected AKT/mTOR pathway components in trametinib-treated and control cells with or without PPP2R1A depletion. (**D**) Cotreatment with AKT inhibitor perifosine in PPP2R1A-depleted A549 cells. Data are shown as means ± SEM for three biological replicate experiments with three technical replicates. (**E**) The impact of PPP2R1A inhibition on A549 cell response to combination of trametinib and mTOR inhibitor temsirolimus. Data are shown as means ± SEM for three biological replicate experiments with three technical replicates. (**F**) Colony growth assay validation of the results shown in (E). Red circle denotes reversal of PPP2R1A inhibition–mediated resistance by temsirolimus combination with the highest trametinib concentration. (**G**) Western blot analysis of selected MAPK and AKT/mTOR pathway components in trametinib- and temsirolimus-treated cells. For selected proteins, different exposures for parts of the same blots are shown in (C). (**H**) MYC expression in PPP2R1A-depleted A549 cells treated with the combination of trametinib (tra) and temsirolimus (tem). Quantification from data is shown as mean fold changes ± SEM for three biological replicate experiments from (G). *$P < 0.05$, two-tailed t test. (**I**) Representative image of a clonogenic assay of H358 cells overexpressing mutant MYC-S62D or enhanced green fluorescent protein (EGFP) control. The graph represents the mean colony number ± SD relative to the vehicle control, three biological replicates with two technical replicates; two-way analysis of variance (ANOVA) with Dunnett's multiple comparison test, ****$P < 0.0001$. DMSO, dimethyl sulfoxide.

xenograft models. The SMAPs are reengineered derivatives of tricyclic neuroleptics. Both tricyclic phenothiazines and the SMAPs directly bind to PPP2R1A (*11*, *36*, *37*), and either mutation of the putative SMAP target-binding site on PPP2R1A or overexpression of viral PIP SV40 small t antigen abrogates the anticancer activities of SMAPs (*11*). Notably, all of the KRAS-mutant lung cancer cell lines overexpressing PIPs (fig. S1C) showed a DT-061 sensitivity profile similar to H460 cells (fig. S4A), where PP2A was inhibited because of PPP2R1A E64D mutation, which should not interfere with SMAP binding based on structural analysis (*11*). These results suggest that cells with prominent PIP overexpression are as addicted to PP2A inhibition as the PP2A mutated cells. Further, the results show that the clinically relevant PP2A inactivation mechanism caused by PIP overexpression in lung cancer cells can be overcome by administration of SMAPs. In addition, CIP2A overexpression did not confer further DT-061 resistance (fig. S4, B and C), suggesting that these cells are already saturated for CIP2A-mediated PP2A inhibition. Finally, in the context of mTOR/AKT signaling as the mechanism of MEKi resistance resulting from PP2A inhibition, SMAP DT-061 inhibits AKT and RPS6K signaling in H358 cells (*38*). We confirmed that the DT-061 + MEKi combination potently inhibited the identified MEKi resistance mechanism (probed by p-AKT and MYC antibodies) in KRAS-mutant lung cancer cell lines H358 and H441 (fig. S4D). Thus, SMAPs are suitable for testing the translational impact of PP2A reactivation in combination with MEKi.

AZD6244 is a potent MEKi used in clinical lung cancer trials. In colony growth experiments, we used DT-061 and AZD6244 in KRAS-mutant H441 and H358 cell lines. Both DT-061 and AZD6244 showed dose-dependent inhibition of colony growth as single agents in both of the cell lines (Fig. 4, A and B). In addition, doses of DT-061 and AZD6244 that alone did not affect colony growth resulted in a very apparent combinatorial activity (Fig. 4, A and B). The cytotoxic activity of the combination was mostly due to DT-061 because AZD6244 failed to induce significant caspase-3/7 activity at the 24-hour time point even at the highest concentration of 10 μM, whereas DT-061 treatment induced a dose-dependent caspase-3/7 activation (fig. S4, E and F). When both drugs were used at a concentration of 10 μM, DT-061 enhanced the apoptosis response in both of the cell lines (Fig. 4C).

We recently demonstrated that the capacity of DT-061 to inhibit H358 xenograft growth was dependent on drug binding to PPP2R1A (*11*). Therefore, we first tested the combinatorial activity of DT-061 and AZD6244 on xenograft growth by using these cells. Assessed by inhibition of the tumor volume, both DT-061 and AZD6244 showed single-agent activity, but their combination was significantly more efficient than either of the compounds alone ($P < 0.0001$; fig. S4G). Similar results were obtained with H441 xenografts ($P < 0.0063$; fig. S4H). To consider this therapeutic strategy for further clinical development, we also assessed the xenograft data in terms of response evaluation criteria in solid tumors (RECIST). With both cell lines, AZD6244 monotherapy resulted in a partial response with about half of the tumors, whereas most of the mice treated with DT-061 alone had progressive disease (Fig. 4, D to F). However, all mice treated with the combination of DT-061 and AZD6244 showed at least a partial response, and one H358 xenograft demonstrated a complete response (Fig. 4, D to F). We analyzed the tumor tissue for tumor cell proliferation, apoptosis, and endogenous MYC expression. The additive effect of MEK inhibition and PP2A reactivation was also evident at the level of tumor cell proliferation and apoptosis, measured by percentages of proliferating cell nuclear antigen (PCNA)– and terminal deoxynucleotidyl transferase–mediated deoxyuridine triphosphate nick end labeling (TUNEL)–positive cells in the tumor tissue, respectively (Fig. 4, G and H, and figs. S4, I and J, and S5, A and B). We also confirmed the effect of AZD6244 and DT-061 in inhibiting endogenous MYC expression in drug-treated tumors in vivo (Fig. 4I and fig. S5, C and D). Notably, as reported for SMAPs alone (*11*), the combination of DT-061 and MEKi did not induce any apparent toxicities in the treated mice (fig. S6).

Finally, we used the H358 cells stably transduced with MYC to study whether the identified MYC-mediated MEKi resistance (Fig. 3, H and I) could be overcome in vivo by pharmacological PP2A reactivation. To link the results to the identified AKT-mediated MEKi resistance mechanism, we compared the effects of DT-061 to the combination of AZD6244 with AKT inhibitor MK2206. When using the control H358-GFP cells, both therapy modalities equally inhibited tumor growth over a 20-day follow-up period (Fig. 4J). As expected, on the basis of the in vitro colony growth results (Fig. 3I), the tumors from cells overexpressing MYC grew faster than the control tumors, but again, the two therapies were indistinguishable in their antitumor activity (Fig. 4K). However, overexpression of a MYC mutant S62D, which is resistant to PP2A dephosphorylation–induced proteolytic degradation (*33*, *39*), induced a partial resistance to DT-061, whereas the combination of AZD6244 and MK2206 efficiently inhibited tumor growth (Fig. 4L). These results validate MYC as an important contributor to MEKi resistance induced by PP2A inhibition. Together, these findings demonstrate that PP2A inhibition is a druggable MEKi resistance mechanism in vivo.

DISCUSSION

The targeting of hyperactive MEK elicits promising clinical responses in many cancer types, but rapidly emerging resistance severely compromises its overall clinical benefit. This is largely due to RAF-mediated reactivation of the ERK pathway or collateral activation of other resistance mechanisms (*2*, *21*). Our complementary findings from PPP2R1A and B-subunit siRNA studies and from a KRAS-mutant lung cancer cell line harboring a loss-of-function PPP2R1A mutation demonstrate that sustained PP2A inhibition drives MAPK inhibitor resistance, including resistance to the combination of RAF and MEKis. Notably, the identified MEKi resistance mechanism was not mediated by the known direct effect of PP2A on MEK-ERK regulation (*5*, *11*, *15*), but rather, it is driven by rewiring of kinase signaling upon MEKi treatment to induce collateral AKT/mTOR and MYC activity. Our conclusions are in line with recent in vivo data demonstrating activation of GSK3β, AKT, and mTOR/p70S6K signaling by PPP2R1A mutations in endometrial cancers (*18*) and with the clinical association between PP2A inhibition and increased S6 phosphorylation (*30*) or MYC amplification and expression (*24*, *40*) in human cancers. In cultured cells, PP2A is well known to regulate phosphorylation of AKT (*41*), several mTOR targets including p70 S6K (*42*), as well as MYC (*32*, *39*). Notably, our PPP2R1A knockout results suggest that haploinsufficiency, rather than complete loss of function, impairs PP2A activity enough to alter MEKi sensitivity. Thus, on the basis of our findings together with the previously demonstrated transformation of human

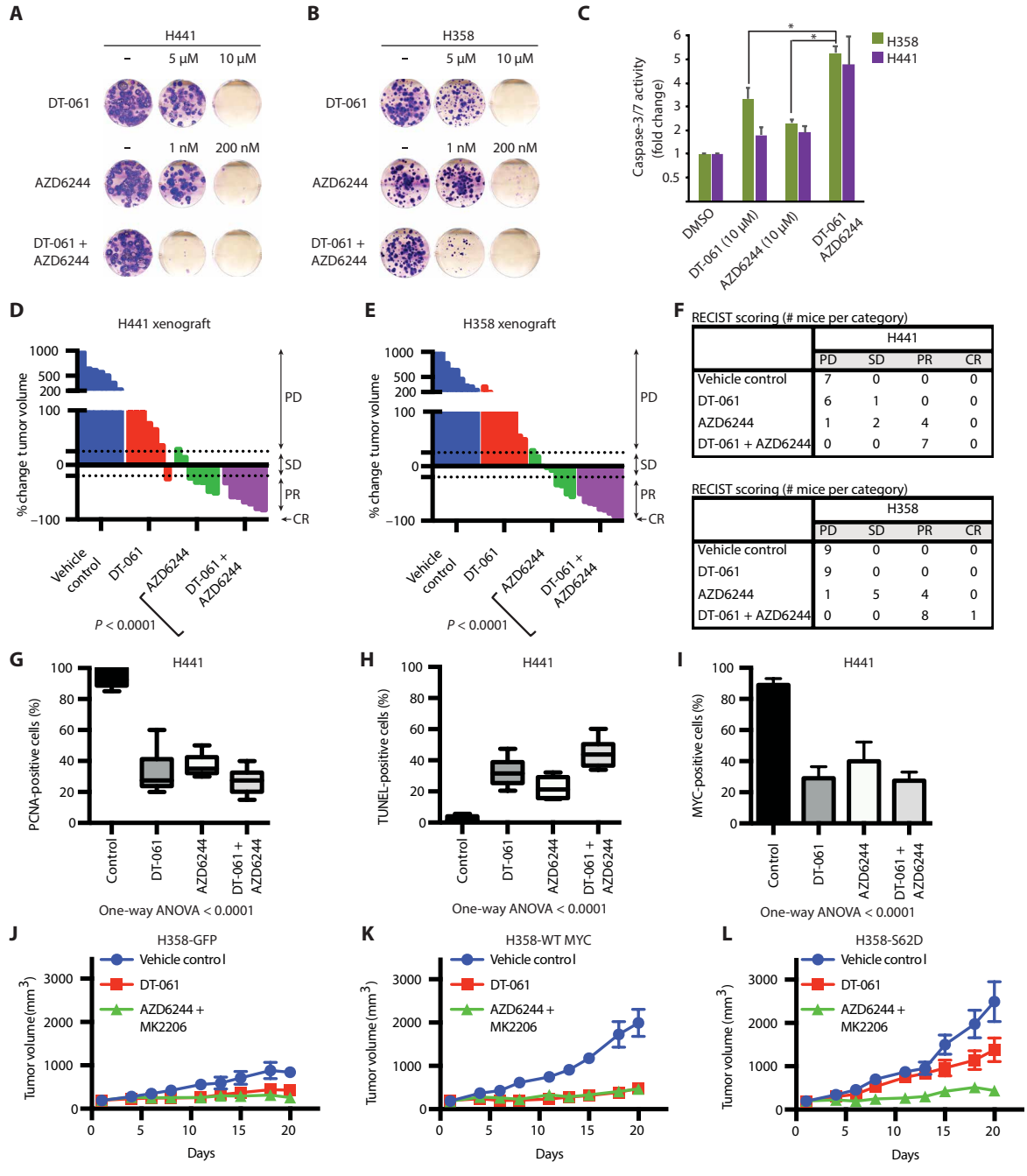

Fig. 4. PP2A inhibition is a druggable MEKi resistance mechanism in vivo. (**A** and **B**) Clonogenic assay of (A) H441 and (B) H358 cells treated with increasing doses of DT-061 (5 μM and 10 μM), AZD6244 (200 nM and 1 μM), or the combination of DT-061 and AZD6244 for 3 weeks. (**C**) Relative caspase-3/7 activity in H358 and H441 cells 24 hours after DT-061, AZD6244, or DT-061 + AZD6244 treatment. Error bars represent SEM of two to three independent experiments. *$P < 0.05$ for both pairs of groups, *t* test. (**D**) H441 cells (5×10^6) were subcutaneously injected into nude mice and allowed to grow to an average of 100 mm^3. Mice were treated by oral gavage with vehicle control ($n = 7$), DT-061 (5 mg/kg; $n = 7$), AZD6244 (25 mg/kg; $n = 7$), or the combination of DT-061 (5 mg/kg) and AZD6244 (25 mg/kg; n=7) for 4 weeks. Graph shows the waterfall plot for H441 xenograft responses. Two-tailed *t* test. (**E**) H358 cells (1×10^7) were subcutaneously injected into nude mice and allowed to grow to an average of 100 mm^3. Mice were treated by oral gavage with vehicle control ($n = 9$), DT-061 (5 mg/kg; $n = 9$), AZD6244 (25 mg/kg; $n = 9$), or the combination of DT-061 and AZD6244 ($n = 9$) for 4 weeks. Graph shows the waterfall plot for H358 xenograft responses. Two-tailed *t* test. PD, progressive disease; SD, stable disease; PR, partial response; CR, complete response. (**F**) Analysis of xenograft data based on RECIST criteria. (**G** to **I**) H441 xenograft tumors were stained for PCNA (proliferation), TUNEL (apoptosis), and MYC. Nuclear staining was quantified as means ± SD (one-way ANOVA). (**J**) Tumor volume growth curves for H358-GFP xenograft. Mice were treated by oral gavage with vehicle control ($n = 8$), DT-061 (5 mg/kg; $n = 8$), or the combination of AZD6244 (24 mg/kg) and MK2206 (6 mg/kg; $n = 8$). Data are shown as means ± SEM. (**K**) Tumor volume growth curves for H358-WT MYC xenograft. Mice were treated by oral gavage with vehicle control ($n = 8$), DT-061 (5 mg/kg; $n = 8$), or the combination of AZD6244 (24 mg/kg) and MK2206 (6 mg/kg; $n = 8$). Data are shown as means ± SEM. (**L**) Tumor volume growth curves for H358-S62D xenograft. Mice were treated by oral gavage with vehicle control ($n = 8$), DT-061 (5 mg/kg; $n = 8$), or the combination of AZD6244 (24 mg/kg) and MK2206 (6 mg/kg; $n = 8$). Data are shown as means ± SEM.

cells by partial PP2A inhibition (*12*) and spontaneous in vivo tumorigenesis driven by PPP2R4 haploinsufficiency (*13*), we postulate that even modest deregulation of PP2A function may be sufficient for activation of collateral resistance pathways and thereby increase tolerance against a number of cancer drugs. From the diagnostic point of view, our findings suggest that PP2A inhibitory mechanisms could be applied as predictive indicators of kinase inhibitor responses. For example, recent evidence in chronic myeloid leukemia has shown that patients with high expression of CIP2A responded only to second-generation tyrosine kinase inhibitors (*43*).

There are limitations to this study. First, the full kinase inhibitor screen with 230 kinase inhibitors was performed only with one cell line. However, the PP2A dependence of sensitivity to 18 kinase inhibitors was confirmed in another KRAS-mutant cell line NCI-H2122, whereas role of PP2A activity in MEKi sensitivity was validated in total in four different KRAS-mutant lung cancer cell lines. Second, although PP2A is known to directly dephosphorylate AKT and to regulate mTOR targets, we could not demonstrate the direct AKT/mTOR pathway targets that were responsible for the pathway activation and MEKi resistance. Third, even though SMAP in combination with MEKi potently inhibited AKT phosphorylation and MYC expression, as well as xenograft growth in both H441 and H358 cells, it remains unclear how mTOR contributed to the MEKi resistance in these cells in vivo.

Beside different combinations of kinase inhibitors, there have been only a few other types of pharmacological approaches to overcome MEKi resistance. Here, we introduce small-molecule PP2A reactivation as an apparently safe approach to target MEKi resistance pathways. PPP2R1A siRNA experiments revealed an important role for PP2A inhibition in preventing efficient cell killing by MAPK combination therapies in vitro. Conversely, PP2A reactivation by DT-061 increased the rate of tumor regression in vivo. Therefore, together with in vitro apoptosis assays, these data indicate that pharmacological PP2A reactivation has a potential to transform MEKi response of KRAS-mutant cells from cytostatic to cytotoxic. The qualitative difference between cytostatic and cytotoxic response is thought to be important with regard to potential development of therapy resistance and regrowth of the tumor (*44*). Moreover, we envision that because of widespread effects of PP2A activity on many of the signaling pathways, combinatorial use of SMAPs may prevent signaling rewiring in kinase inhibitor–treated cancer cells and thereby inhibit development of drug resistance. Future studies should aim to understand whether treatment with SMAPs could prevent establishment of resistance in treatment-naïve cells. Finally, our screen conducted with 230 kinase inhibitors in PP2A-modulated cells provides a resource for further identification of combination therapy strategies, in particular with pharmacological PP2A modulators such as SMAPs (*37*). In addition, our results may help in identification of combination targeting strategies or PP2A-related biomarkers associated with response to these additional drugs. At a more general level, our results emphasize the need for better understanding of phosphatases as key modulators of cancer therapy responses.

MATERIALS AND METHODS

Study design

This study aimed to determine whether PP2A activity affects kinase inhibitor responses of KRAS-mutant lung cancer cells. Initial drug sensitivity screen included 230 kinase inhibitors and was performed in A549 cells depleted for PP2A structural subunit (PPP2R1A) or its endogenous inhibitors (CIP2A and PME-1). In addition to RNAi, PP2A activity was manipulated pharmacologically or by genome editing. Signaling changes after PP2A activity manipulation and treatment with MEKi trametinib were analyzed by quantitative phosphoproteomics. Finally, we assessed the therapeutic potential of pharmacological PP2A activation as a combination therapy with MEKis in mouse xenograft models. For each xenograft, tumor cells were injected subcutaneously into nude mice. Mice were monitored, and tumor volumes were assessed every other day.

Efficacy end points

Mice were followed and tumor volumes were assessed every other day by standard caliper measurement until the tumors reached 1000 mm^3, at which time mice were anesthetized, blood was drawn, and tumors were removed. Tumor volume was estimated every other day by standard caliper measurement ($V = L \times W^2/2$).

Safety end points

Total body weight was monitored twice weekly, and mice were monitored for overall well-being and signs of distress.

Pharmacodynamic end points

Tumors were split for FFPE (formalin-fixed paraffin-embedded) paraffin blocks, RNA isolation, protein isolation, and frozen for analysis of putative biomarkers/targets. Immunohistochemistry (IHC) was performed on the tissues for MYC, PCNA, and TUNEL.

Cell culture and drugs

A549, H460, H358, H441, and H2122 cell lines were obtained from the American Type Culture Collection. HBEC (HBEC3-KT) immortalized by CDK4 and hTERT was described by Ramirez and colleagues (*27*). Dulbecco's modified Eagle's medium (Sigma-Aldrich) was used for A549 and RPMI 1640 (Sigma-Aldrich) for H460, H358, H441, and H2122. All media contained 10% fetal bovine serum (Sigma-Aldrich), 2 mM L-glutamine (Sigma-Aldrich), penicillin (50 IU/ml; Biowest), and streptomycin (50 μg/ml; Biowest). HBEC cells were cultured in keratinocyte serum-free growth medium supplemented with EGF 1-53 and bovine pituitary extract (Thermo Fisher Scientific). SMAP (DT-061) was manufactured as described in (*11*). AZD6244 was purchased from Selleck Chemicals, and all the other drugs were from MedChemExpress. The drugs were diluted in dimethyl sulfoxide and stored at room temperature (DT-061) or −20°C (all other drugs).

Phosphoproteomics

Sample preparation, LC-MS/MS analysis, and the pairwise normalization for label-free quantitative phosphoproteomics were performed according to a previously published protocol (*15*). Each siRNA treatment was performed in triplicates. Samples were collected 72 hours after the transfection and 20 hours after the 100 nM trametinib treatment. ERK and AKT target predictions were performed with NetworKIN (*45*).

Bioinformatics

The numbers of up-regulated phosphopeptides for each gene were substracted from the number of down-regulated phosphopeptides, and the derived difference values were used as PP2A activity index (*23*). The ΔΔDSS was calculated by subtracting the ΔDSS of the PPP2R1A from the summed ΔDSSs of the inhibitor proteins. Drugs were then ranked by ΔΔDSS. Enrichment scores for selected drug groups in the ranked lists were calculated similarly to GSEA (*46*).

Drug sensitivity testing and drug responses

For the high-throughput DSRT analyses, cells were transfected 3 days before plating them on the drug-containing plates. Depending on the cell line, 500 to 1000 cells were plated on 384-well plate wells based on their proliferative capacity (determined by saturation of the CellTiter-Glo readout). The subsequent analyses were carried out as described previously (*22*). ΔDSS (*28*) was calculated by comparing the response of each siRNA-depleted sample to the average of control samples. For colony formation assays involving siRNA transfections, 3000 cells in each well on six-well plate were plated 1 day after transfections together with drugs, and the assays were performed as described previously (*15*). To differentiate between cytostatic and cytotoxic effect in Figs. 2I and 3F, 20,000 cells per well were plated on 48-well plates 1 day after transfection with drugs and grown for 4 days. The cells were stained with crystal violet similarly to the colony formation assay, and the coverage was assessed visually. For the AZD62244 + DT-061 experiments, cells were seeded at 1000 cells per well and allowed to grow for 3 weeks in the presence of vehicle control or increasing concentrations of the drugs. For the trametinib + DT-061 experiments, cells were seeded at 1000 cells per well and allowed to grow for 2 weeks in the presence of vehicle control or increasing concentrations of the drugs. Cells were fixed, stained with crystal violet, and quantified using ImageJ. For cell viability and apoptosis assays, cells were plated in 96-well plates. After incubation at 37°C for 24 hours, the cultures were treated with the drugs for 3 days, and the proportion of viable and apoptotic cells was determined by WST1 assay (Roche) and Caspase-Glo 3/7 Assay (Promega), respectively, according to the manufacturer's recommendations.

Mouse models and treatment studies

All animal experiments were approved by the Institutional Animal Care and Use Committee (IACUC) at Icahn School of Medicine at Mount Sinai (IACUC protocol number, IACUC-2013-1426). Animal use and care were in strict compliance with institutional guidelines, and all experiments were conformed to the relevant regulatory standards established by Icahn School of Medicine at Mount Sinai. For xenograft studies, H358 (1×10^7 cells) or H441 (5×10^6 cells) cells were injected into the right flank of 6- to 8-week-old male BALB/c nu/nu mice (Charles River). When tumor volumes reached an average of 100 mm^3, mice were randomized to treatment groups, and tumor volume was assessed by caliper measurement every other day throughout the study. Mice were treated by gavage with vehicle control, AZD6244 (25 mg/kg), SMAP (5 mg/kg), or SMAP in combination with AZD6244. The body weights of mice were recorded weekly, and the percentage of body weights during treatment was calculated as weight at each time point/initial weight × 100. Animals were observed for signs of toxicity (mucous diarrhea, abdominal stiffness, or weight loss). Blood and tumor tissue were harvested 2 hours after the final dose of the treatment study. Tumors were both formalin-fixed for IHC and snap-frozen in liquid nitrogen for immunoblotting.

Statistical analysis

Statistical analyses were performed using JMP Pro (version 12.0 for Windows software, SAS Institute Inc.) and GraphPad PRISM (version 6, Graphpad software Inc.). All statistical tests were two-sided and considered significant at $P < 0.05$. Continuous variables were compared using *t* test, one-way ANOVA, and two-way ANOVA. When necessary for the assumption of normal distribution, transformations were performed for continuous variables. When performing multiple comparisons, alpha level was adjusted by Šidák's (*47*) or Dunnett's correction, or FDR was controlled by the Benjamini-Hochberg procedure (*48*). Frequencies were calculated for categorical data and compared using chi-square test. IC_{50} was estimated for partial (cytostatic) drug responses by fitting a five-parameter logistic function to mean viability values of replicate experiments normalized to cytotoxicity control and untreated cells in each experiment.

SUPPLEMENTARY MATERIALS

www.sciencetranslationalmedicine.org/cgi/content/full/10/450/eaaq1093/DC1
Materials and Methods
Fig. S1. PP2A activity restricts KRAS-mutant lung cancer cell line proliferative potential.
Fig. S2. MEKi resistance in KRAS-mutant lung cancer cells by PP2A inhibition.
Fig. S3. PPP2R1A inhibition drives MEKi resistance by increased AKT/mTOR pathway activities.
Fig. S4. Validation of PP2A inhibition as a druggable MEKi resistance mechanism in vivo.
Fig. S5. Analysis of xenograft tissues with respect to proliferation, apoptosis, and MYC protein expression.
Fig. S6. Pharmacological PP2A activation does not induce weight loss in animals.
Table S1. A549 cell DSRT.
Table S2. Validation drug screen in NCI-H460 and NCI-H2122 cells.
Table S3. Oligonucleotide sequences and antibody information.

REFERENCES AND NOTES

1. A. Tibau, C. Molto, A. Ocana, A. J. Templeton, L. P. Del Carpio, J. C. Del Paggio, A. Barnadas, C. M. Booth, E. Amir, Magnitude of clinical benefit of cancer drugs approved by the US Food and Drug Administration. *J. Natl. Cancer Inst.* **110**, 486–492 (2018).
2. R. Mandal, S. Becker, K. Strebhardt, Stamping out RAF and MEK1/2 to inhibit the ERK1/2 pathway: An emerging threat to anticancer therapy. *Oncogene* **35**, 2547–2561 (2016).
3. I. Ntanasis-Stathopoulos, G. Fotopoulos, I.-G. Tzanninis, E. A. Kotteas, The emerging role of tyrosine kinase inhibitors in ovarian cancer treatment: A systematic review. *Cancer Invest.* **34**, 313–339 (2016).
4. O. Kauko, J. Westermarck, Non-genomic mechanisms of protein phosphatase 2A (PP2A) regulation in cancer. *Int. J. Biochem. Cell Biol.* **96**, 157–164 (2018).
5. D. Perrotti, P. Neviani, Protein phosphatase 2A: A target for anticancer therapy. *Lancet Oncol.* **14**, e229–e238 (2013).
6. W. C. Hahn, S. K. Dessain, M. W. Brooks, J. E. King, B. Elenbaas, D. M. Sabatini, J. A. DeCaprio, R. A. Weinberg, Enumeration of the simian virus 40 early region elements necessary for human cell transformation. *Mol. Cell. Biol.* **22**, 2111–2123 (2002).
7. A. Rangarajan, S. J. Hong, A. Gifford, R. A. Weinberg, Species- and cell type-specific requirements for cellular transformation. *Cancer Cell* **6**, 171–183 (2004).
8. R. Ruediger, J. Ruiz, G. Walter, Human cancer-associated mutations in the Aα subunit of protein phosphatase 2A increase lung cancer incidence in Aα knock-in and knockout mice. *Mol. Cell. Biol.* **31**, 3832–3844 (2011).
9. A. Laine, H. Sihto, C. Come, M. T. Rosenfeldt, A. Zwolinska, M. Niemelä, A. Khanna, E. K. Chan, V.-M. Kähäri, P.-L. Kellokumpu-Lehtinen, O. J. Sansom, G. I. Evan, M. R. Junttila, K. M. Ryan, J.-C. Marine, H. Joensuu, J. Westermarck, Senescence sensitivity of breast cancer cells is defined by positive feedback loop between CIP2A and E2F1. *Cancer Discov.* **3**, 182–197 (2013).
10. G. Walter, R. Ruediger, Mouse model for probing tumor suppressor activity of protein phosphatase 2A in diverse signaling pathways. *Cell Cycle* **11**, 451–459 (2012).
11. J. Sangodkar, A. Perl, R. Tohme, J. Kiselar, D. B. Kastrinsky, N. Zaware, S. Izadmehr, S. Mazhar, D. D. Wiredja, C. M. O'Connor, D. Hoon, N. S. Dhawan, D. Schlatzer, S. Yao, D. Leonard, A. C. Borczuk, G. Gokulrangan, L. Wang, E. Svenson, C. C. Farrington, E. Yuan, R. A. Avelar, A. Stachnik, B. Smith, V. Gidwani, H. M. Giannini, D. McQuaid, K. McClinch, Z. Wang, A. C. Levine, R. C. Sears, E. Y. Chen, Q. Duan, M. Datt, S. Haider, A. Ma'ayan, A. DiFeo, N. Sharma, M. D. Galsky, D. L. Brautigan, Y. A. Ioannou, W. Xu, M. R. Chance, M. Ohlmeyer, G. Narla, Activation of tumor suppressor protein PP2A inhibits KRAS-driven tumor growth. *J. Clin. Invest.* **127**, 2081–2090 (2017).
12. W. Chen, J. D. Arroyo, J. C. Timmons, R. Possemato, W. C. Hahn, Cancer-associated PP2A Aα subunits induce functional haploinsufficiency and tumorigenicity. *Cancer Res.* **65**, 8183–8192 (2005).
13. W. Sents, B. Meeusen, P. Kalev, E. Radaelli, X. Sagaert, E. Miermans, D. Haesen, C. Lambrecht, M. Dewerchin, P. Carmeliet, J. Westermarck, A. Sablina, V. Janssens, PP2A inactivation mediated by *PPP2R4* haploinsufficiency promotes cancer development. *Cancer Res.* **77**, 6825–6837 (2017).

14. C. Lambrecht, L. Libbrecht, X. Sagaert, P. Pauwels, Y. Hoorne, J. Crowther, J. V. Louis, W. Sents, A. Sablina, V. Janssens, Loss of protein phosphatase 2A regulatory subunit B56δ promotes spontaneous tumorigenesis in vivo. *Oncogene* **37**, 544–552 (2018).
15. O. Kauko, T. D. Laajala, M. Jumppanen, P. Hintsanen, V. Suni, P. Haapaniemi, G. Corthals, T. Aittokallio, J. Westermarck, S. Y. Imanishi, Label-free quantitative phosphoproteomics with novel pairwise abundance normalization reveals synergistic RAS and CIP2A signaling. *Sci. Rep.* **5**, 13099 (2015).
16. N. Naetar, V. Soundarapandian, L. Litovchick, K. L. Goguen, A. A. Sablina, C. Bowman-Colin, P. Sicinski, W. C. Hahn, J. A. DeCaprio, D. M. Livingston, PP2A-mediated regulation of Ras signaling in G2 is essential for stable quiescence and normal G1 length. *Mol. Cell* **54**, 932–945 (2014).
17. X. Zhou, B. L. Updegraff, Y. Guo, M. Peyton, L. Girard, J. E. Larsen, X. J. Xie, Y. Zhou, T. H. Hwang, Y. Xie, J. Rodriguez-Canales, P. Villalobos, C. Behrens, I. I. Wistuba, J. D. Minna, K. A. O'Donnell, PROTOCADHERIN 7 acts through SET and PP2A to potentiate MAPK signaling by EGFR and KRAS during lung tumorigenesis. *Cancer Res.* **77**, 187–197 (2017).
18. D. Haesen, L. Abbasi Asbagh, R. Derua, A. Hubert, S. Schrauwen, Y. Hoorne, F. Amant, E. Waelkens, A. Sablina, V. Janssens, Recurrent *PPP2R1A* mutations in uterine cancer act through a dominant-negative mechanism to promote malignant cell growth. *Cancer Res.* **76**, 5719–5731 (2016).
19. Q.-Z. Dong, Y. Wang, X.-J. Dong, Z.-X. Li, Z.-P. Tang, Q.-Z. Cui, E.-H. Wang, CIP2A is overexpressed in non-small cell lung cancer and correlates with poor prognosis. *Ann. Surg. Oncol.* **18**, 857–865 (2011).
20. A. Kaur, O. V. Denisova, X. Qiao, M. Jumppanen, E. Peuhu, S. U. Ahmed, O. Raheem, H. Haapasalo, J. Eriksson, A. J. Chalmers, P. Laakkonen, J. Westermarck, PP2A inhibitor PME-1 drives kinase inhibitor resistance in glioma cells. *Cancer Res.* **76**, 7001–7011 (2016).
21. M. P. Smith, C. Wellbrock, Molecular pathways: Maintaining MAPK inhibitor sensitivity by targeting nonmutational tolerance. *Clin. Cancer Res.* **22**, 5966–5970 (2016).
22. T. Pemovska, M. Kontro, B. Yadav, H. Edgren, S. Eldfors, A. Szwajda, H. Almusa, M. M. Bespalov, P. Ellonen, E. Elonen, B. T. Gjertsen, R. Karjalainen, E. Kulesskiy, S. Lagström, A. Lehto, M. Lepistö, T. Lundán, M. M. Majumder, J. M. L. Marti, P. Mattila, A. Murumägi, S. Mustjoki, A. Palva, A. Parsons, T. Pirttinen, M. E. Rämet, M. Suvela, L. Turunen, I. Västrik, M. Wolf, J. Knowles, T. Aittokallio, C. A. Heckman, K. Porkka, O. Kallioniemi, K. Wennerberg, Individualized systems medicine strategy to tailor treatments for patients with chemorefractory acute myeloid leukemia. *Cancer Discov.* **3**, 1416–1429 (2013).
23. O. Kauko, S. Y. Imanishi, E. Kulesskiy, T. D. Laajala, L. Yetukuri, A. Laine, M. Jumppanen, P. Haapaniemi, L. Ruan, B. Yadav, V. Suni, T. Varila, G. Corthals, J. Reimand, K. Wennerberg, T. Aittokallio, J. Westermarck, Rules for PP2A-controlled phosphosignalling and drug responses. bioRxiv:271841 (2018).
24. M. Niemelä, O. Kauko, H. Sihto, J.-P. Mpindi, D. Nicorici, P. Pernilä, O.-P. Kallioniemi, H. Joensuu, S. Hautaniemi, J. Westermarck, CIP2A signature reveals the MYC dependency of CIP2A-regulated phenotypes and its clinical association with breast cancer subtypes. *Oncogene* **31**, 4266–4278 (2012).
25. A. Kaur, J. Westermarck, Regulation of protein phosphatase 2A (PP2A) tumor suppressor function by PME-1. *Biochem. Soc. Trans.* **44**, 1683–1693 (2016).
26. J. Wang, J. Okkeri, K. Pavic, Z. Wang, O. Kauko, T. Halonen, G. Sarek, P. M. Ojala, Z. Rao, W. Xu, J. Westermarck, Oncoprotein CIP2A is stabilized via interaction with tumor suppressor PP2A/B56. *EMBO Rep.* **18**, 437–450 (2017).
27. R. D. Ramirez, S. Sheridan, L. Girard, M. Sato, Y. Kim, J. Pollack, M. Peyton, Y. Zou, J. M. Kurie, J. M. DiMaio, S. Milchgrub, A. L. Smith, R. F. Souza, L. Gilbey, X. Zhang, K. Gandia, M. B. Vaughan, W. E. Wright, A. F. Gazdar, J. W. Shay, J. D. Minna, Immortalization of human bronchial epithelial cells in the absence of viral oncoproteins. *Cancer Res.* **64**, 9027–9034 (2004).
28. B. Yadav, T. Pemovska, A. Szwajda, E. Kulesskiy, M. Kontro, R. Karjalainen, M. M. Majumder, D. Malani, A. Murumägi, J. Knowles, K. Porkka, C. Heckman, O. Kallioniemi, K. Wennerberg, T. Aittokallio, Quantitative scoring of differential drug sensitivity for individually optimized anticancer therapies. *Sci. Rep.* **4**, 5193 (2014).
29. A. Kaur, A. Elzagheid, E.-M. Birkman, T. Avoranta, V. Kytölä, E. Korkeila, K. Syrjänen, J. Westermarck, J. Sundström, Protein phosphatase methylesterase-1 (PME-1) expression predicts a favorable clinical outcome in colorectal cancer. *Cancer Med.* **4**, 1798–1808 (2015).
30. J. Routila, J.-A. Mäkelä, H. Luukkaa, I. Leivo, H. Irjala, J. Westermarck, A. Mäkitie, S. Ventelä, Potential role for inhibition of protein phosphatase 2A tumor suppressor in salivary gland malignancies. *Genes Chromosomes Cancer* **55**, 69–81 (2016).
31. T. M. Pitts, S. L. Davis, S. G. Eckhardt, E. L. Bradshaw-Pierce, Targeting nuclear kinases in cancer: Development of cell cycle kinase inhibitors. *Pharmacol. Ther.* **142**, 258–269 (2014).
32. M. R. Junttila, P. Puustinen, M. Niemelä, R. Ahola, H. Arnold, T. Böttzauw, R. Ala-aho, C. Nielsen, J. Ivaska, Y. Taya, S. L. Lu, S. Lin, E. K. Chan, X. J. Wang, R. Grenman, J. Kast, T. Kallunki, R. Sears, V. M. Kähäri, J. Westermarck, CIP2A inhibits PP2A in human malignancies. *Cell* **130**, 51–62 (2007).
33. M. Janghorban, A. S. Farrell, B. L. Allen-Petersen, C. Pelz, C. J. Daniel, J. Oddo, E. M. Langer, D. J. Christensen, R. C. Sears, Targeting c-MYC by antagonizing PP2A inhibitors in breast cancer. *Proc. Natl. Acad. Sci. U.S.A.* **111**, 9157–9162 (2014).
34. T. K. Hayes, N. F. Neel, C. Hu, P. Gautam, M. Chenard, B. Long, M. Aziz, M. Kassner, K. L. Bryant, M. Pierobon, R. Marayati, S. Kher, S. D. George, M. Xu, A. Wang-Gillam, A. A. Samatar, A. Maitra, K. Wennerberg, E. F. Petricoin III, H. H. Yin, B. Nelkin, A. D. Cox, J. J. Yeh, C. J. Der, Long-term ERK inhibition in *KRAS*-mutant pancreatic cancer Is associated with MYC degradation and senescence-like growth suppression. *Cancer Cell* **29**, 75–89 (2016).
35. P. Kalev, M. Simicek, I. Vazquez, S. Munck, L. Chen, T. Soin, N. Danda, W. Chen, A. Sablina, Loss of PPP2R2A inhibits homologous recombination DNA repair and predicts tumor sensitivity to PARP inhibition. *Cancer Res.* **72**, 6414–6424 (2012).
36. A. Gutierrez, L. Pan, R. W. J. Groen, F. Baleydier, A. Kentsis, J. Marineau, R. Grebliunaite, E. Kozakewich, C. Reed, F. Pflumio, S. Poglio, B. Uzan, P. Clemons, L. VerPlank, F. An, J. Burbank, S. Norton, N. Tolliday, H. Steen, A. P. Weng, H. Yuan, J. E. Bradner, C. Mitsiades, A. T. Look, J. C. Aster, Phenothiazines induce PP2A-mediated apoptosis in T cell acute lymphoblastic leukemia. *J. Clin. Invest.* **124**, 644–655 (2014).
37. C. M. O'Connor, A. Perl, D. Leonard, J. Sangodkar, G. Narla, Therapeutic targeting of PP2A. *Int. J. Biochem. Cell Biol.* **96**, 182–193 (2018).
38. D. D. Wiredja, M. Ayati, S. Mazhar, J. Sangodkar, S. Maxwell, D. Schlatzer, G. Narla, M. Koyuturk, M. R. Chance, Phosphoproteomics profiling of nonsmall cell lung cancer cells treated with a novel phosphatase activator. *Proteomics* **17**, 1700214 (2017).
39. A. S. Farrell, R. C. Sears, MYC degradation. *Cold Spring Harb. Perspect. Med.* **4**, (2014).
40. A. Khanna, C. Böckelman, A. Hemmes, M. R. Junttila, J.-P. Wiksten, M. Lundin, S. Junnila, D. J. Murphy, G. I. Evan, C. Haglund, J. Westermarck, A. Ristimäki, MYC-dependent regulation and prognostic role of CIP2A in gastric cancer. *J. Natl. Cancer Inst.* **101**, 793–805 (2009).
41. S. Andrabi, O. V. Gjoerup, J. A. Kean, T. M. Roberts, B. Schaffhausen, Protein phosphatase 2A regulates life and death decisions via Akt in a context-dependent manner. *Proc. Natl. Acad. Sci. U.S.A.* **104**, 19011–19016 (2007).
42. R. T. Peterson, B. N. Desai, J. S. Hardwick, S. L. Schreiber, Protein phosphatase 2A interacts with the 70-kDa S6 kinase and is activated by inhibition of FKBP12-rapamycinassociated protein. *Proc. Natl. Acad. Sci. U.S.A.* **96**, 4438–4442 (1999).
43. C. M. Lucas, R. J. Harris, A. K. Holcroft, L. J. Scott, N. Carmell, E. McDonald, F. Polydoros, R. E. Clark, Second generation tyrosine kinase inhibitors prevent disease progression in high-risk (high CIP2A) chronic myeloid leukaemia patients. *Leukemia* **29**, 1514–1523 (2015).
44. T. Ni Chonghaile, K. A. Sarosiek, T.-T. Vo, J. A. Ryan, A. Tammareddi, V. del G. Moore, J. Deng, K. C. Anderson, P. Richardson, Y.-T. Tai, C. S. Mitsiades, U. A. Matulonis, R. Drapkin, R. Stone, D. J. DeAngelo, D. J. McConkey, S. E. Sallan, L. Silverman, M. S. Hirsch, D. R. Carrasco, A. Letai, Pretreatment mitochondrial priming correlates with clinical response to cytotoxic chemotherapy. *Science* **334**, 1129–1133 (2011).
45. R. Linding, L. J. Jensen, A. Pasculescu, M. Olhovsky, K. Colwill, P. Bork, M. B. Yaffe, T. Pawson, NetworKIN: A resource for exploring cellular phosphorylation networks. *Nucleic Acids Res.* **36**, D695–D699 (2008).
46. A. Subramanian, P. Tamayo, V. K. Mootha, S. Mukherjee, B. L. Ebert, M. A. Gillette, A. Paulovich, S. L. Pomeroy, T. R. Golub, E. S. Lander, J. P. Mesirov, Gene set enrichment analysis: A knowledge-based approach for interpreting genome-wide expression profiles. *Proc. Natl. Acad. Sci. U.S.A.* **102**, 15545–15550 (2005).
47. Z. Šidák, Rectangular confidence regions for the means of multivariate normal distributions. *J. Am. Stat. Assoc.* **62**, 626–633 (1967).
48. Y. Benjamini, Y. Hochberg, Controlling the false discovery rate: A practical and powerful approach to multiple testing. *J. R. Stat. Soc.* **57**, 289–300 (1995).

Acknowledgments: We thank the Turku Proteomics Facility, the Turku Cell Imaging Core and Viral Vector Facility at Turku Centre for Biotechnology, and the High Throughput Biomedicine Unit at the Institute for Molecular Medicine Finland for instrument support and technical assistance. We thank T.-K. Mattila, R. Tohme, and A. Heinonen for their valuable technical help, S. Mazhar and A. Perl for generating the MYC and shB-subunit stable cells, respectively, and S. Imanishi for expert help in phosphoproteomics. J. Shay and E. Verschuren are thanked for sharing the HBEC-KT and lung cancer cells, respectively. We also acknowledge a number of colleagues for their critical feedback on the manuscript. **Funding:** Academy of Finland (grants 269862, 272437, 292611, and 310507 for T.A., 277293 for K.W., and 252572 and 294850 for J.W.), Cancer Society of Finland (J.W., T.A., and K.W.), Sigrid Juselius Foundation (J.W., T.A., and K.W.), Foundation of Finnish Cancer Institute (J.W.), Instrumentarium Science Foundation (O.K.), Finnish Cultural Foundation (O.K.), and R01 CA181654 (G.N.). **Author contributions:** O.K., J.W., and G.N. conceived the study. O.K., J.W., T.A., K.W., G.N., J.S., C.M.O., and M.O designed the experiments. M.O. designed and synthesized the SMAP compounds. O.K., C.M.O., E.K., J.S., A.A., S.I., A.P., P.H., M.M., and T.V performed the experiments. L.Y., B.Y., T.D.L., E.K., and O.K. performed the bioinformatics analyses. J.W., G.N., K.W., and T.A. supervised the study and provided funding. O.K and J.W. wrote the manuscript; T.A., K.W., G.N., J.S., C.M.O., A.A., and S.I. contributed to the writing and editing of the manuscript. **Competing interests:** The Icahn School of Medicine at Mount Sinai and Case Western Reserve University on behalf of the authors G.N. and M.O. have filed patents covering composition of matter on the small

molecules disclosed here for the treatment of human cancer and other diseases and for methods of use for using these small-molecule PP2A activators in combination with MEKi for the treatment of human cancer (patent number: 9540358, "Tricyclic compounds as anticancer agents"). Rappta Therapeutics LLC has licensed this intellectual property for the clinical and commercial development of this series of small-molecule PP2A activators. The authors G.N. and M.O. have an ownership interest in Rappta Therapeutics LLC. M.O. received research support from and was a consultant for Dual Therapeutics LLC. **Data and materials availability:** Raw MS data are available via ProteomeXchange with identifier PXD009900. Used research material is available by request from the corresponding author or from commercial sources when applicable.

Submitted 3 October 2017
Resubmitted 21 April 2018
Accepted 8 June 2018
Published 18 July 2018
10.1126/scitranslmed.aaq1093

Citation: O. Kauko, C. M. O'Connor, E. Kulesskiy, J. Sangodkar, A. Aakula, S. Izadmehr, L. Yetukuri, B. Yadav, A. Padzik, T. D. Laajala, P. Haapaniemi, M. Momeny, T. Varila, M. Ohlmeyer, T. Aittokallio, K. Wennerberg, G. Narla, J. Westermarck, PP2A inhibition is a druggable MEK inhibitor resistance mechanism in KRAS-mutant lung cancer cells. *Sci. Transl. Med.* **10**, eaaq1093 (2018).

Science Translational Medicine

PP2A inhibition is a druggable MEK inhibitor resistance mechanism in KRAS-mutant lung cancer cells

Otto Kauko, Caitlin M. O'Connor, Evgeny Kulesskiy, Jaya Sangodkar, Anna Aakula, Sudeh Izadmehr, Laxman Yetukuri, Bhagwan Yadav, Artur Padzik, Teemu Daniel Laajala, Pekka Haapaniemi, Majid Momeny, Taru Varila, Michael Ohlmeyer, Tero Aittokallio, Krister Wennerberg, Goutham Narla and Jukka Westermarck

Sci Transl Med **10**, eaaq1093.
DOI: 10.1126/scitranslmed.aaq1093

An oncogene's enemy is our friend

Inhibitors of oncogenic kinases such as MEK are becoming increasingly common as an approach to treating cancer, but these drugs' effectiveness is often short-lived, as tumors develop resistance. Phosphatases, a class of proteins whose activity counteracts that of kinases, are not routinely targeted by cancer therapies but may offer an alternative approach to treatment in some cases. In particular, Kauko *et al*. determined that the loss of a phosphatase called PP2A can play a major role in resistance to MEK inhibition in lung cancer. The authors also selected a compound that activates PP2A and demonstrated that it can effectively combine with a MEK inhibitor and overcome drug resistance in multiple mouse models of human lung cancer.